DESIGN AND EXPERIMENT OF A COMBINED ROOT-CUTTING AND DITCHING DEVICE
/
组合式切根开沟装置的设计与试验

Xuening ZHANG, Yong YOU *), Decheng WANG *), Jie LV [1]
China Agricultural University, College of Engineering, Beijing / China
Tel: +86 10 010-62737977; +86 10 010-62737208; E-mail: youyong@cau.edu.cn; wdc@cau.edu.cn
Corresponding authors: Yong You, Decheng Wang

ABSTRACT

To improve the ditching performance of high-firmness grassland, a bionic root cutter based on the contour curve model of Prosopocoilus astacoides' jaw was designed, as well as a grassland root-cutting and ditching device combining the bionic root cutter with the core-share opener. The grassland ditching experiment investigated the horizontal working resistance, ditching stability, and soil disturbance of the three ditching parts. According to the trial results, when the core-share opener was used for ditching in high-firmness grassland, the ditching stability was poor, the working resistance was high, and the grassland was severely damaged. Compared with the independent configuration of the core-share opener, the ditching performance can be significantly improved by installing a root cutter in front of the core-share opener, and the effect of installing the bionic root cutter was better than that of an ordinary triangular root cutter. When the ditching depth was 5 cm, 10 cm, and 15 cm, the ditching stability coefficient of the root-cutting and ditching device increased by 16.67%, 9.54%, and 6.18%, respectively, the horizontal working resistance reduced by 58.73%, 28.15%, and 19.84%, respectively, and the soil disturbance area reduced by 30.58%, 23.73%, and 20.21%, respectively.

摘要

为提高高坚实度草地的开沟性能，依据前锹甲上颚轮廓曲线模型，设计了一种新型仿生切根刀，并研制了一种将仿生切根刀与芯铧式开沟器相组合的草地切根开沟装置。通过草地开沟试验，对三种开沟部件的水平工作阻力、开沟稳定性以及草地扰动情况进行了比较分析。试验结果表明，芯铧式开沟器在高坚实度草地进行开沟作业时，其开沟稳定性较差、耕作阻力较大，对草地破坏严重。相较于芯铧式开沟器单独配置，在其前方加装切根刀可以显著提升开沟性能，且加装仿生切根刀比普通三角切根刀的效果更佳；加装仿生切根刀的芯铧式开沟器在 5cm、10cm、15cm 开沟深度时的开沟稳定性系数分别提高了 16.67%、9.54%、6.18%，水平工作阻力分别降低了 58.73%、28.15%、19.84%，土壤扰动面积分别降低了 30.58%、23.73%、20.21%。

INTRODUCTION

The subterranean roots of *Leymus Chinensis* are intertwined with soil to form the soil–root composites. The formation of the composites enhanced grassland firmness and decreased grassland permeability, which became the direct cause of natural grassland degradation in China (*You et al., 2011; You et al., 2011; He et al., 2016*). When ditching on natural grassland, the traditional ditching parts frequently fail to create the desired ditching effect. The ditching resistance is excessive, and the grassland vegetation and roots are seriously damaged. At the same time, the excessive disturbance created by traditional ditching parts makes the grassland susceptible to wind erosion, resulting in the deterioration of natural grassland. Therefore, developing ditching parts appropriate for high-firmness grassland is critical.

The current ditching parts of natural grassland are mostly improved by traditional farming parts, such as hoe-shovel openers, arrow-shovel openers, wing-shovel openers, core-share openers, disc openers, etc. (*Zhao et al., 2014*). Its application in farmland is quite mature, but it has great limitations as a ditching part of natural grassland (*He et al., 2015*).

---

[1] *Xuening Zhang, Ph.D. Stud. Eng; Yong You, As. Prof. Ph.D. Eng.; Decheng Wang, Prof. Ph.D. Eng.; Jie Lv, M.S. Stud. Eng.*

Scholars have studied the ditching of high-firmness grassland and reached some conclusions. *He et al. (2019)* investigated the coupling failure characteristics including surface disturbance and profile, disturbed cross-section area, soil over-turning rate, and coupling forces between the soil layer of natural grassland and selected passive subsoiler-type openers. *Liang et al. (2021)* achieved steady ditching of shallow grassland layer using a double-disc opener.

To address problematic ditching in high-firmness grassland, this paper designed a root-cutting and ditching device that combines the bionic root cutter with the core-share opener. It could ditch the grassland based on the grooves cut out by the root-cutting operation. The ditching performance of three ditching parts: core-share opener, triangular root cutter + core-share opener, bionic root cutter + core-share opener were compared and analyzed. The findings of the study can be used to generate fresh ideas and references for the design of ditching parts of natural grassland.

MATERIALS AND METHODS
- **Experimental site description**

The grassland ditching experiment was conducted on September 26, 2020. The experiment site was located in typical natural grassland in the Chabei district of Hebei province (41°28'31.649″N, 115°1'28.733″E). A flat topography and uniform grassland vegetation characterized the trial region. Leymus Chinensis was the dominant grass species in this area. The average of physical parameters of grassland obtained by field measurements were as follows: water content 9.98 %, bulk density 1.41 g/cm^3, firmness 2864 KPa, and porosity 50.47%.

- **Design of bionic root cutter**

Prosopocoilus astacoides feeds on the nutrient solution found in the plant's rhizome. The developed jaw and sharp edges of the *Prosopocoilus astacoides* enable it to cut the plant rhizome to access the nutrient solution. In this paper, the jaw of *Prosopocoilus astacoides* was taken as the research object, and its contour curve was fitted to the edge of the root cutter for the optimization design of the root cutter. The jaw contour of the *Prosopocoilus astacoides* was shown in Fig. 2 (a). Import the image of the *Prosopocoilus astacoides*' jaw into the MATLAB software, take points successively for the jaw contour of the *Prosopocoilus astacoides* by tracing points, and recording the coordinate values of each point (*Zhao et al., 2017*).

The fitting precision of the curve cannot be guaranteed using the low-order polynomial fitting method due to a large number of data points obtained, while the high-order polynomial fitting method would increase the difficulty of calculation and even distortion. Therefore, the full jaw contour curve of *Prosopocoilus astacoides* was obtained using the piecewise polynomial fitting method (*Liu et al., 2014*). The inner and outer contour curves of the *Prosopocoilus astacoides*' jaw were split into five stages for fitting in this article. The fitting equations of each stage were shown in table 1, and the determination coefficient for all equations were more than 0.9, indicating that the fitting effect of all equations was good.

Table 1

The fitting equations of each stage

Each stage		Fitting equation	Determination coefficient
Inner contour curve	Stage 1	$y = 0.106x^3-21.04x^2+1396x-3.086e+04$	0.996
	Stage 2	$y = 7.32x^3-1.38e+03x^2+8.68e+04x-1.82e+06$	0.999
	Stage 3	$y = -3.27x^3+626x^2-3.99e+04x+8.49e+05$	0.985
	Stage 4	$y = -0.0087x^3+1.9x^2-1.4e+02x+3.7e+03$	0.992
	Stage 5	$y = -0.00022x^3+0.074x^2-8.8x+3.8e+02$	0.978
Outer contour curve	Stage 1	$y = -25x^3+1.4e+03x^2-2.5e+04x+1.5e+05$	0.998
	Stage 2	$y = -0.021x^3+1.8x^2-52x+6.2e+02$	0.985
	Stage 3	$y = -0.0032x^3+0.36x^2-16x+3.1e+02$	0.992
	Stage 4	$y = -0.0013x^3+0.19x^2-11x+2.6e+02$	0.998
	Stage 5	$y = -4.3e-05x^3+0.018x^2-2.5x+1.3e+02$	0.935

The fitting curves of the inner and outer contours of the *Prosopocoilus astacoides*' jaw were shown in Fig. 1.

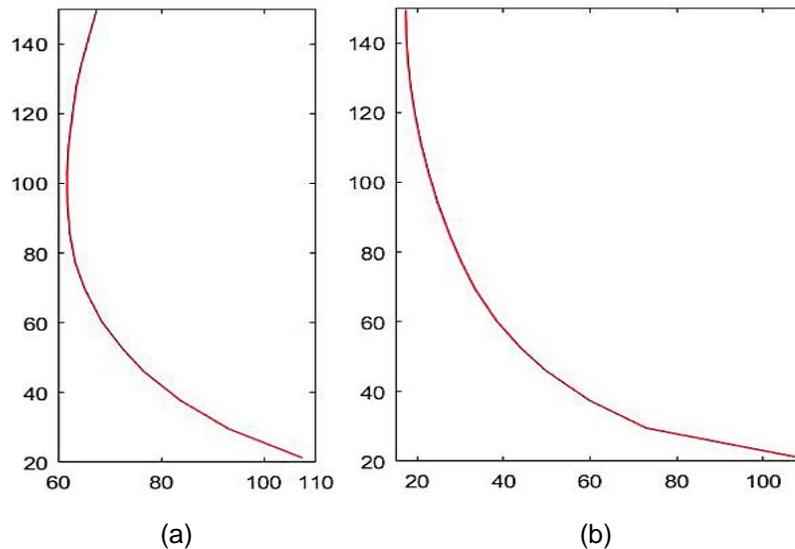(a)   (b)

Fig. 1 - The fitting curves of the inner and outer contours of the *Prosopocoilus astacoides*' jaw:
(a) Fitting curve of the inner contour;   (b) Fitting curve of the outer contour

The simulation model of the bionic root cutter was established based on the fitting equations of the *Prosopocoilus astacoides*' inner and outer contour, as shown in Fig. 2 (b). The bionic root cutter model was scaled up and manufactured, as shown in Fig. 2 (c). According to the requirements of the grassland root-cutting operation and the processing size of the test bench, the penetration angle of the root cutter was set to 28.6 °, the penetration gap angle was set to 5.2 °, the blade length was set to 200 mm, the handle width was set to 50 mm, and the total length of the root cutter was set to 775 mm.
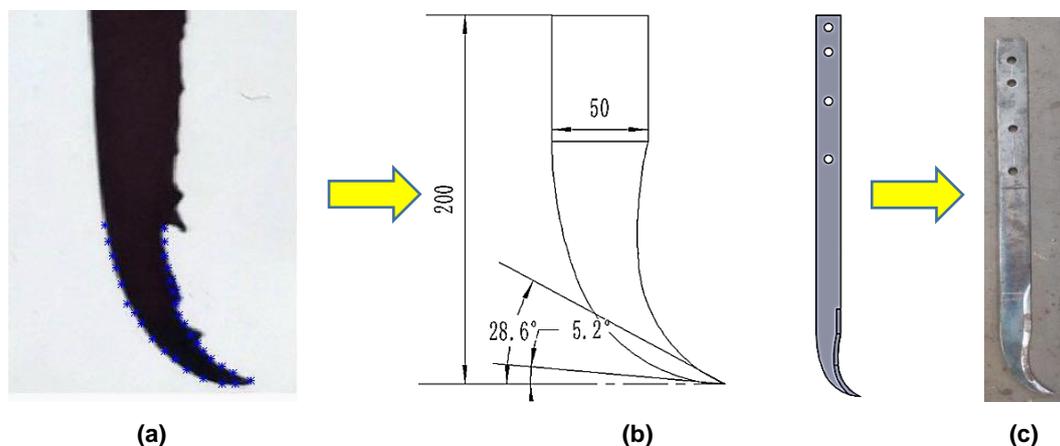

(a)   (b)   (c)

Fig. 2 - The bionic root cutter: (a) The jaw contour of the *Prosopocoilus astacoides*;
(b) Fitting contour and simulation model of root cutter; (c) Physical tool

● **Design of core-share opener**

The core-share opener is simple in structure and reliable in operation, and its main structure includes core-share, share handle, and wing plate. It can squeeze the soil on both sides along the ditch gap cut by the root cutter and expand it to seed ditches, which can better cooperate with the root cutter to complete the root-cutting and ditching operation.

The parameters of the core-share opener were selected by referring to the agricultural machinery design manual and other literature (*CAAMS, 2007; Cao et al., 2016*). A small penetration angle lengthens the share-tip and reduces the opener's strength, while a large penetration angle increases the opener's working resistance. Therefore, the opener's penetration angle α was set to 24°. A small penetration gap angle lowers the penetration performance of the opener, while a large penetration gap angle readily leads to an uneven ditch bottom. Therefore, the penetration gap angle ε of the opener was set to 9 °. Due to the small size of forage seeds, the width B of the opener was set to 40 mm.

The chamfer angle affects the slippage of the grassland soil, and the opener's chamfer angle γ was set to 60° to reduce soil disturbance. The ridge curvature radius affects the structural compactness of the opener, and the ridge curvature radius R of the opener was set to 300 mm. A high share-height increases the working resistance of the opener, and the share-height H of the opener was set to 110 mm. The structural parameters and physical objects of the core-share opener were shown in Fig. 3.
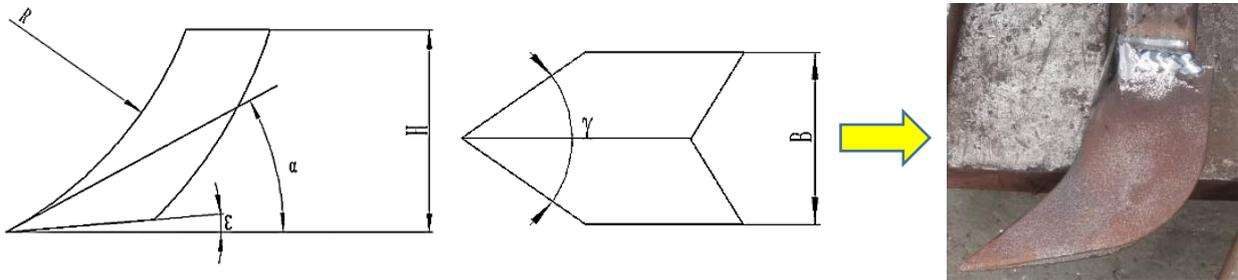

Fig. 3 - The core-share opener

● **Combined root-cutting and ditching device**

The combined root-cutting and ditching device was shown in Fig. 4. The main structure includes a traction frame, bionic root cutter, core-share opener, depth-limiting wheel, pressure sensor, and data collector. The test bench was linked with a tractor by three-point hydraulic suspension frames, and the power output shaft provides the operating power.
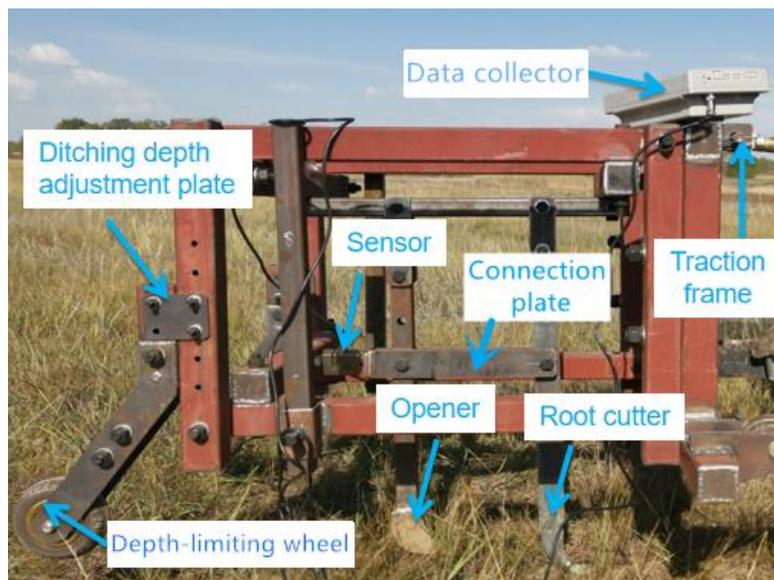

Fig. 4 - Combined root-cutting and ditching device

The connection plate connected the bionic root cutter to the core-share opener, and the machine penetrated the soil layer through its gravity. The pressure sensor was installed directly behind the connection plate, and received the horizontal working resistance from the ditching parts, which was then recorded by the data collector. To satisfy varied test requirements, the device can be equipped with the bionic root cutter and the core-share opener at the same time or individually. The ditching depth was adjusted by the depth-limiting wheel and ditching depth adjustment plate.

● **Experimental procedure and calculation**

To investigate the operating effectiveness of the combined root-cutting and ditching device, the grassland ditching experiment was carried out. There were three kinds of ditching parts: core-share opener, bionic root cutter + core-share opener, triangular root cutter + core-share opener. The triangular root cutter's penetration angle, penetration gap angle, and blade length were consistent with those of the bionic root cutter. The structural parameters of the triangular root cutter were shown in Fig. 5.

The device was operated at a forward speed of 1.08±0.14 km/h pulled by the tractor moving at a slow speed of No.2 level (*He et al., 2020*). The operating depth was 5 cm, 10 cm, and 15 cm, respectively. The evaluation indicators of the experiment were ditching stability coefficient, horizontal working resistance, and soil disturbance area.
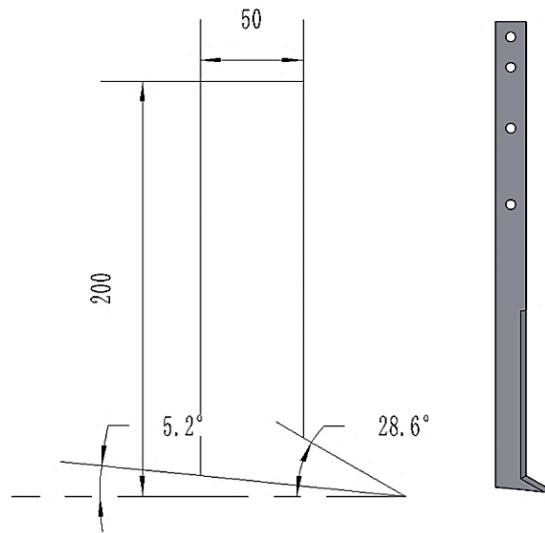

Fig. 5 - The structural parameters of the triangular root cutter

The ditching stability coefficient was used to describe the stability of working depth during the tillage movements of the ditching parts (*Pan et al., 2016; Yang et al., 2019*), calculated as follows:

$$S = \sqrt{\frac{\sum_{i=1}^{n}(h_i - h)^2}{N-1}} \tag{1}$$

$$V = \frac{S}{h} \times 100\% \tag{2}$$

$$U = (1-V) \times 100\% \tag{3}$$

where:

    U is the ditching stability coefficient;

    V is the coefficient of variation;

    S is the standard deviation of depth;

    h is the average value of depth;

    h_i is the measured depth value at the point i;

    N and n are the numbers of the measurement points.

The working resistance curve of each ditching part in the horizontal direction was collected by the pressure sensor. The stable stage of the curve was selected and its average value was calculated as the horizontal working resistance of each ditching part (*Hasimu et al., 2014; Ding et al., 2017*).

The soil disturbance area was utilized to assess the disturbance of each ditching part on natural grassland. The pit contour and ridge contour constitute the disturbance contour of the soil cross-section (*Huang et al., 2016*), as shown in Fig. 6.

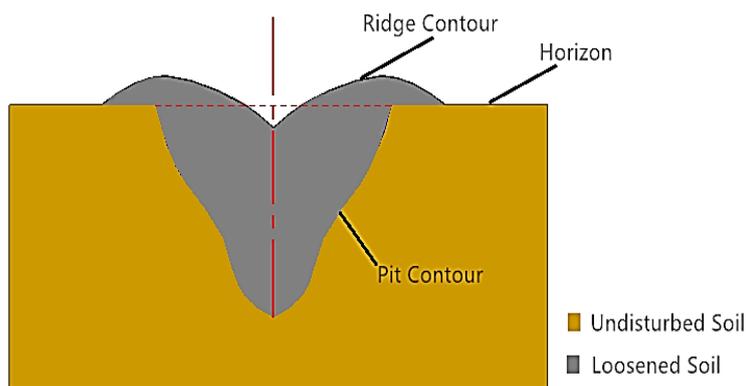The gray figure contour is the soil cross-section disturbance contour, and its area is the soil disturbance area.

Fig. 6 - Schematic diagram of the soil cross-section disturbance contour

The disturbed area of soil was measured by a profiler, as shown in Fig. 7. The profiler was composed of a connection ruler, strip slider, and fixed block. The strip slider could slide up and down along the connection ruler, and was held in place by the fixed block. The soil cross-section disturbance contour measured by the profiler was plotted on the coordinate paper, and the soil disturbance area was calculated.
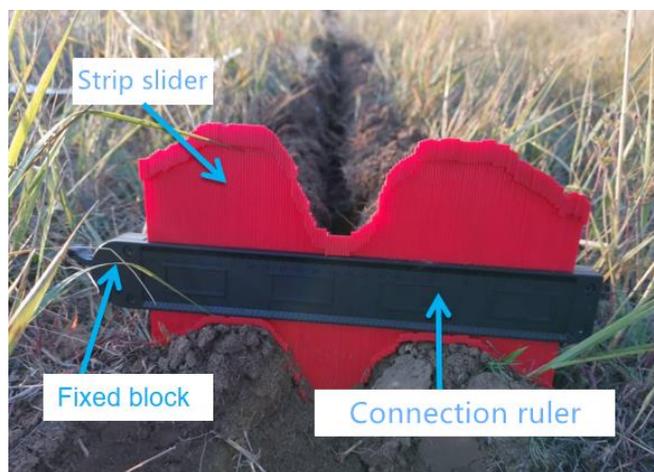

Fig. 7 - Determination of soil disturbance area

RESULTS

- **Ditching stability**

After each group's ditching test was completed, the actual ditching depth was measured every 1 m for a total of 8 times. The ditching stability coefficient was computed once the measurement was completed. The computation results were shown in Table 2. The ditching stability coefficient increased with the ditching depth increasing.

Table 2

Ditching stability coefficient

Type of ditching parts	Design ditching depth /cm	Actual ditching depth /cm	Relative error/%	Ditching stability coefficient /%
Core-share opener	5	3.7±0.966	26	71.82
	10	7.0±1.365	30	79.22
	15	12.1±1.581	19.3	86.10
Triangular root cutter + Core-share opener	5	4.6±0.994	8	76.65
	10	8.1±1.172	19	84.53
	15	12.3±1.612	18	86.03
Bionic root cutter + Core-share opener	5	5.1±0.545	2	88.49
	10	9.7±1.022	3	88.76
	15	13.9±1.003	7.3	92.28

The relative error between the actual and design ditching depth of the core-share opener was the largest. The relative error of the three ditching depths was more than 19%, making it impossible to satisfy the expected requirements of the design ditching depth. The ditching stability of the core-share opener was the worst, and its ditching stability coefficient varied obviously at different ditching depths, which was greatly affected by the ditching depth.

When the ditching depth was 5 cm or 10 cm, installing the triangular root cutter in front of the core-share opener increased the ditching stability coefficient by 4.83% and 5.31%, respectively. When the ditching depth was deepened to 15 cm, the ditching stability coefficients of the two became nearly identical. Under this ditching depth, installing the triangular root cutter would not help the core-share opener improve ditching stability.

The ditching stability increased even further when the bionic root cutter was installed in front of the core-share opener. The ditching stability coefficient increased by 16.67%, 9.54%, and 6.18% for ditching depths of 5 cm, 10 cm, and 15 cm, respectively. The ditching stability of the core-share opener could still be increased at a deeper ditching depth by installing the bionic root cutter. At varied ditching depths, the relative error between the actual and design ditching depths was less than 8%, and the ditching stability coefficients were all more than 88%. Furthermore, its ditching stability coefficients changed little at different ditching depths, implying that ditching depth has less of an influence on ditching stability.

- **Horizontal working resistance**

The horizontal working resistance of each ditching part at different ditching depths was shown in Fig. 8. The horizontal working resistance of ditching parts increased with the actual ditching depth increase. At the same ditching depth, the horizontal working resistance of the core-share opener was the highest. By installing a root cutter in front of the core-share opener, the horizontal working resistance of the ditching part considerably decreased, and the drag reduction effect of installing the bionic root cutter was superior to the triangular root cutter.

Each curve showed a high degree of fit with the R^2 value exceeding 0.96. Because the actual ditching depth of each ditching part varied, the horizontal working resistance of each ditching part was calculated by the fitting curve for comparative analysis when the ditching depth was 5 cm, 10 cm, and 15 cm. Compared with the single configuration of the core-share opener, when the ditching depth was 5 cm, 10 cm, and 15 cm, installing the triangular root cutter reduced the horizontal working resistance by 22.26%, 7.32%, and 3.25%, respectively, while installing the bionic root cutter reduced it by 58.73%, 28.15%, and 19.84%, respectively. The drag reduction effect of installing a root cutter steadily diminished with the ditching depth increasing. When the ditching depth was 15 cm, the drag reduction effect of installing the triangular root cutter was limited, while the drag reduction effect of installing the bionic root cutter was still close to 20%. The bionic root cutter still has a significant drag reduction effect when the ditching depth was deep.
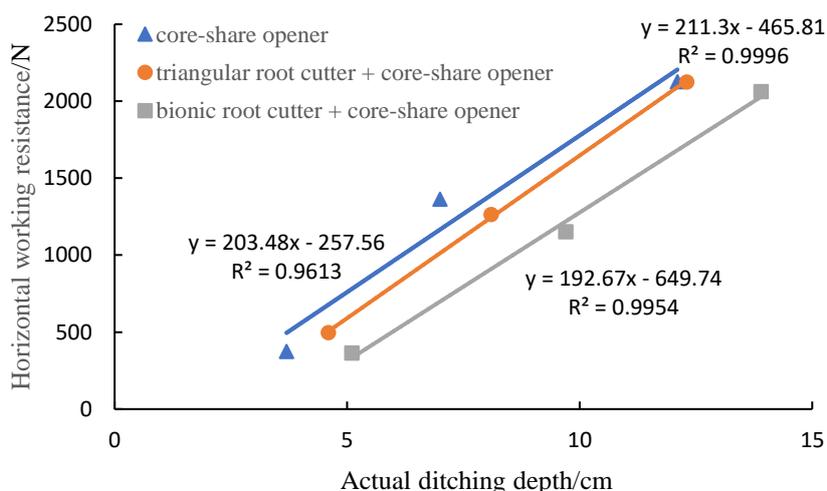

Fig. 8 - Horizontal working resistance of ditching parts

- **Soil disturbance area**

The soil disturbance area of each ditching part at different ditching depths was shown in Fig. 9. The soil disturbance area of each ditching part increased with the actual ditching depth increase. At the same ditching depth, the soil disturbance area of the core-share opener was the highest.

Installing the root cutter in front of the core-share opener considerably reduced the soil disturbance area, and the soil disturbance area caused by installing the bionic root cutter was significantly smaller than that generated by installing the triangular root cutter.

Each curve showed a high degree of fit with the R^2 value exceeding 0.98. Because the actual ditching depth of each ditching part varied, the soil disturbance area of each ditching part was calculated by the fitting curve for comparative analysis when the ditching depth was 5 cm, 10 cm, and 15 cm. Compared with the single configuration of the core-share opener, installing the triangular root cutter reduced the soil disturbance area by 23.09%, 9.46%, and 2.45% when the ditching depth was 5 cm, 10 cm, and 15 cm, respectively, while installing the bionic root cutter reduced it by 30.58%, 23.73%, and 20.21%, respectively. When the ditching depth was shallow, installing the triangular root cutter or the bionic root cutter in front of the core-share opener could significantly reduce the soil disturbance area. However, when the ditching depth was deepened to 10 cm, the effect of installing the triangular root cutter was considerably reduced. When the ditching depth was deepened to 15 cm, the soil disturbance area was reduced by just 2.45% by installing the triangular root cutter, but it was reduced by 20.21% by installing the bionic root cutter. Even though the ditching depth was deep, the bionic root cutter greatly reduced the soil disturbance area.
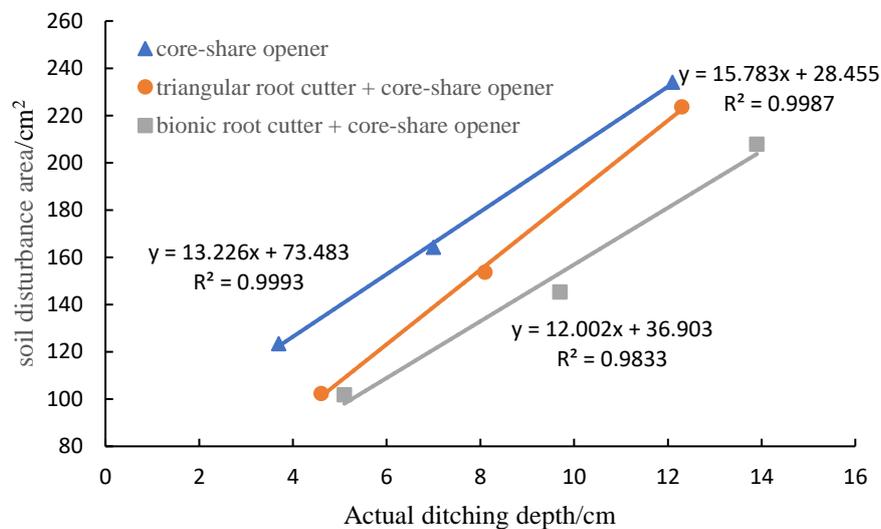
Fig. 9 - Soil disturbance area of ditching parts

The disturbance of the grassland surface by the ditching parts was shown in Fig. 10. The grassland surface displayed the phenomenon of big clods being overturned along the furrow after the ditching operation was completed by the core-share opener. The roots of the grassland were turned out with the soil, inflicting significant damage to the natural grassland. After the ditching operation of the core-share opener equipped with the triangular root cutter or the bionic root cutter was completed, no large clods were overturned and the damage to the grassland was insignificant.
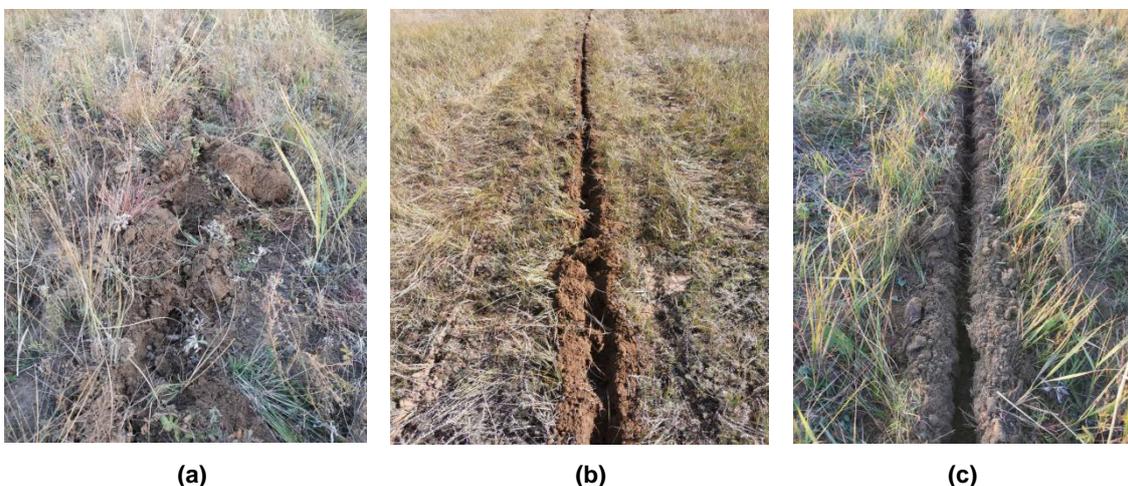
(a)   **(b)**   **(c)**

Fig. 10 - Disturbance of grassland surface: (a) Core-share opener;
(b) Triangular root cutter + Core-share opener; (c) Bionic root cutter + Core-share opener

As shown in Fig. 11 (a), the core-share opener squeezed out the soil through the core-share during the ditching operation. Due to its large width and poor soil-breaking performance, the core-share opener not only destroyed the grassland vegetation and roots seriously but also created big clods on the surface of the grassland. During the operation of the combined root-cutting and ditching device, the root cutter cut out the grooves on the surface of the grassland and cut off the roots at the same time. Then, the core-share opener squeezed the soil with the grooves cut out by the root cutter. The operation process reduced the pulling of the core-share opener on the roots, so the combined root-cutting and ditching device has less disturbance during ditching operation, as shown in Fig. 11 (b).

(a)   **(b)**

Fig. 10 - Coupling procedure between the grassland surface and ditching parts:
(a) Core-share opener; (b) Root cutter + Core-share opener

CONCLUSIONS

(1) Because of its poor ditching stability, high ditching resistance, and substantial damage to grassland vegetation and roots, the core-share opener was not suitable for grassland ditching alone. The combined root-cutting and ditching device improved ditch stability and reduced the working resistance and grassland damage.

(2) When the ditching depth was 5 cm, 10 cm, and 15 cm, compared with the core-share opener, the combined root-cutting and ditching device increased the ditching stability by 16.67%, 9.54%, and 6.18%, respectively, and the horizontal working resistance reduced by 58.73%, 28.15%, and 19.84%, respectively, and the soil disturbance area decreased by 30.58%, 23.73%, and 20.21%, respectively.

(3) The ditching depth has a great influence on the ditching effect of the ditching parts. When the ditching depth was deep, the ditching stability of the ditching parts improved, but the horizontal working resistance of the ditching parts and the disturbance damage to the grassland increased. When the ditching depth was shallow, the ditching effect could be significantly improved by installing the triangular root cutter or the bionic root cutter in front of the core-share opener. When the ditching depth was deep, the ditching effect improved by installing the triangular root cutter was limited, but the ditching effect could still be significantly improved by installing the bionic root cutter.

ACKNOWLEDGEMENT

REFERENCES

[1] CAAMS (Chinese Academy of Agricultural Mechanization Sciences), (2007). *Agricultural machinery design manual.* pp. 377, Beijing/China.

[2] Cao X., Zhao S., Liu H., Yang Y., Zhou Y., (2016). Design and Experiment of Winter-wheat No-tillage Seeder for Inter-planting (垄间套播冬小麦免耕播种机设计与试验). *Journal of Agricultural Mechanization Research*, Vol. 38, pp. 157-161, Heilongjiang/China.

[3] Ding Q., Ge S., Ren J., Li Y., He R., (2017). Characteristics of Subsoiler Traction and Soil Disturbance in Paddy Soil (水稻土深松阻力与土壤扰动效果研究). *Transactions of the Chinese Society for Agricultural Machinery*, Vol. 48, pp. 47-56, Beijing/China.

[4]   Hasimu A., Chen Y., (2014). Soil disturbance and draft force of selected seed openers. *Soil & Tillage Research*, Vol. 140, pp. 48-54, Amsterdam/Netherlands.

[5]   He, C., Wang, D., Wang, G., You Y., Liang F., Liu L., Shao C., (2015). The development of grassland mechanical restoration technology research (天然草地机械化改良技术研究进展). *Journal of Agricultural Mechanization Research*, Vol. 37, pp. 258-263, Heilongjiang/China. (in Chinese with English abstract)

[6]   He C., You Y., Wang D., He G., Wu H., Ye B., (2019). Effect of tine geometry on penetration resistance during vertical movement on natural grassland. *INMATEH-Agricultural Engineering*, Vol. 59, pp.19-26, Bucharest / Romania.

[7]   He C., You Y., Wang D., Wang G., Wu H., Gong S., (2016). Mechanical characteristics of soil-root composite and its influence factors in degenerated grassland (退化草地复合体力学特性与影响因素研究). *Transactions of the Chinese Society for Agricultural Machinery*, Vol. 47, pp. 79-89, Beijing/China.

[8]   He C, You Y, Wang D, Wu H., Ye B., (2020). An experimental investigation of soil layer coupling failure characteristics on natural grassland by passive subsoiler-type openers. *INMATEH - Agricultural Engineering*, Vol. 60, pp. 293-302, Bucharest / Romania.

[9]   Huang Y., Hang C., Yuan M., Wang B., Zhu R., (2016). Discrete Element Simulation and Experiment on Disturbance Behavior of Subsoiling (深松土壤扰动行为的离散元仿真与试验). *Transactions of the Chinese Society for Agricultural Machinery*, Vol. 47, pp. 80-88, Beijing/China.

[10]   Liang F., Wang D., You Y., Wang G., Wang Y., Zhang X., Feng J., (2021). Design and experiment of root-cutter with fertilization and reseeding compound remediation machine for grassland (草地切根施肥补播复式改良机设计与试验). *Journal of Jilin University (Engineering and Technology Edition)*, pp. 1-10, Jilin/China.

[11]   Liu X., Wang Y., (2014). Research of Automatically Piecewise Polynomial Curve-fitting Method Based on Least-square Principle (基于最小二乘法的自动分段多项式曲线拟合方法研究). *Science Technology and Engineering*, Vol. 14, pp. 55-58, Beijing/China.

[12]   Pan S., Cao Z., Yang Y., Zhao W., (2016). The Design n of Furrow Opener Based on Discrete Element Method (基于离散元法的芯铧式开沟器设计). *Journal of Agricultural Mechanization Research*, pp. 23-27, Heilongjiang/China.

[13]   Yang W., Wu B., Peng Z., Tan S., (2019). Estimation of the Operation Quality of Vertical Helix Furrow Openers Based on the Discrete Element Method (基于离散元法立式螺旋开沟器开沟质量的评价). *Journal of Southwest University(Natural Science)*, Vol. 41, pp. 1-7, Chongqing/China.

[14]   You Y., Wang D., Liu J., (2011). A device for mechanical remediation of degraded grasslands. *Soil & Tillage Research*, Vol. 118, pp. 1-10, Amsterdam/Netherlands.

[15]   You Y., Wang D., Wang G., (2011). 9QP-830 Soil-gashing and Root-cutting Mechanism (9QP-830 型草地破土切根机). *Transactions of the Chinese Society for Agricultural Machinery*, Vol. 42, pp. 61-67, Beijing/China.

[16]   Zhao S., Liu H., Tan H., Cao X., Zhang X., Yang Y., (2017). Design and performance experiment of opener based on bionic sailfish head curve (仿旗鱼头部曲线型开沟器设计与性能试验). *Transactions of the Chinese Society of Agricultural Engineering (Transactions of the CSAE)*, Vol. 33, pp. 32-39, Beijing/China.

[17]   Zhao J., Yang X., Zhou J., Liu L., Yang H., (2014). Analysis the Current Situation about Furrow Opener and its Performance Test Device (播种机开沟器及其性能测试装置的现状分析). *Journal of Agricultural Mechanization Research*, Vol. 1, pp. 238-241, Beijing/China.